scientific reports

Check for updates

OPEN

Peptidylarginine deiminase 2 contributes to pathogenesis in trinitrobenzenesulfonic acid-induced colitis through macrophage extracellular trap-independent pathways

Hiroyuki Yasuda[1]✉, Michiko Saito[2], Shusaku Hayashi[1] & Shinichi Kato[1]

Peptidylarginine deiminase 2 (PAD2) is an enzyme that converts arginine to citrulline and is involved in diseases, such as Alzheimer's diseases, fibrosis and cancer. However, its role in inflammatory bowel disease remains unclear. In this study, we investigated the pathogenic effects of PAD2 on inflammatory bowel disease using a trinitrobenzene sulfonic acid (TNBS)-induced murine colitis model. PAD2-deficient (PAD2KO) mice were generated using CRISPR/Cas9-mediated genomic editing. TNBS injection resulted in body weight loss, extensive colonic erosion, and ulceration in wild-type (WT) mice. However, these responses were significantly attenuated in PAD2KO mice. TNBS-induced increases in myeloperoxidase activity, inflammatory cytokine expression, and macrophage extracellular traps (METs) induction in the colon were significantly reduced in PAD2KO. Furthermore, METs were triggered in peritoneal macrophages obtained from WT mice by A23187 and phorbol myristate acetate, and notably, these responses were not abolished in PAD2KO mice. Moreover, inflammatory cytokine expression and M1 macrophage polarization in peritoneal macrophages obtained from PAD2KO mice was lower than that in peritoneal macrophages from WT mice. Overall, PAD2 contributes to the pathogenesis of TNBS-induced colitis by regulating inflammatory cytokine expression in macrophages through METs-independent pathways. Therefore, PAD2 is a promising target for treating inflammatory bowel disease.

Keywords Peptidylarginine deiminase 2, Colitis, Macrophage, Extracellular traps, Cytokines

Inflammatory bowel disease (IBD), including Crohn's disease (CD) and ulcerative colitis (UC), are chronic inflammatory diseases caused by the dyshomeostasis of the intestinal immune responses and dysfunction of the intestinal epithelial barrier[1–3]. However, the factors contributing to IBD remain incompletely known. The dyshomeostasis of intestinal immune responses or abnormal immune responses are known to be initiated by the activation of immune cells, such as neutrophils, macrophages, and T-lymphocytes[4–6]. In particular, the immune response of $CD4^+$-helper T cell (Th) plays a pivotal role in IBD pathogenesis; cytokines associated with Th1/Th17-mediated immune responses are important in the pathogenesis of CD; and cytokines associated with Th2-mediated immune response are important in the pathogenesis of UC[7]. Interestingly, several studies have demonstrated that extracellular traps (ETs), a type of innate immune response, contribute to IBD pathogenesis through various mechanisms, including impairment of the intestinal epithelial barrier and persistent inflammation induced by macrophage activation[8,9]. Therefore, understanding Th1/2/17-related cytokines and ETs-centered intestinal immune responses may provide effective therapeutic targets for ameliorating IBD.

ET formation is a phenomenon in which immune cells release chromatin fibers containing granule content, such as myeloperoxidase (MPO)[10]. In particular, chromatin decondensation, which is induced by

[1]Division of Pathological Sciences, Department of Pharmacology and Experimental Therapeutics, Kyoto Pharmaceutical University, Kyoto 6078414, Japan. [2]Bio-Science Research Center, Kyoto Pharmaceutical University, Kyoto 6078414, Japan. ✉email: yasuda20@mb.kyoto-phu.ac.jp

histone citrullination, is known to play an important role in DNA release[11]. These ETs are induced not only by neutrophils but also by macrophages[12], and are involved in the pathogenesis of inflammatory diseases, including autoimmune diseases[13,14], renal disease[15], cancer[16] and sepsis[17]. Among these, macrophage extracellular traps (METs) are reported to be induced by microbial infection[18] and are associated with tumor invasion[19] and renal injury[20]. Furthermore, ETs are involved in cardiovascular disease and atherosclerosis by inducing thrombus formation[12,21,22]. Thus, ETs derived from neutrophils or macrophages may be involved in the pathogenesis and exacerbation of inflammatory diseases. Many studies have shown that the induction of neutrophil extracellular traps (NETs) is mediated by reactive oxygen species (ROS) and/or histone citrullination[11,23]. In recent years, it has been known that various factors, including not only bacteria and viruses but also DAMPs, cytokines, and activated platelets, have been reported to be involved in the NET induction as well as in ROS induction and histone citrullination[15]. Although histone citrullination-dependent NETs are induced via activation of peptidylarginine deaminase 4 (PAD4)[24], which is abundant in neutrophils, the detailed mechanism underlying METs induction remains unclear. METs are reported to be induced through PAD2 and PAD4, which are known to be expressed in macrophages[25], and are involved in rheumatoid arthritis[26], however, it is still unclear whether PAD2 is involved in ET induction. Moreover, PAD2 is widely distributed in mammals and contributes to protein citrullination similarly to PAD4. Despite its association with PAD4, the role of PAD2 in the pathogenesis of IBD has not been clarified.

Recently, we reported that NETs induction through activated PAD4 is involved in experimental colitis[27]. Our results showed that the pathogenesis of trinitrobenzene sulfonic acid (TNBS)-induced colitis is inhibited in PAD4KO mice and that NETs are induced by PAD4 activity. Similarly, the pharmacological effects of Cl-amidine, a pan-PAD inhibitor, and DNase I, an ET inhibitor, suppress the pathogenesis of colitis, suggesting that PAD activity and ET induction may be important in TNBS-induced colitis. Although several studies have reported that NETs and PAD4, an inducing factor, are involved in the pathogenesis of IBD[8], the involvement of PAD2 remains unclear. Elucidating the role of both PAD4 and PAD2 can help clarify the importance of citrullinating proteins in the pathogenesis of IBD. In this study, we aimed to elucidate, for the first time, the involvement of PAD2 activity or METs induction in IBD using PAD2KO mice in TNBS-induced colitis model.

Materials and methods

Animals

Male C57BL/6 mice (8–9 weeks), weighing 21–26 g, were purchased from Japan SLC Inc. (Shizuoka). PAD2-deficient (PAD2KO) mice were generated by deleting *PAD2* genomic DNA, including part of exon 2, from C57BL/6 mice using the CRISPR/Cas9 system (Fig. 1a); the deletion was confirmed by DNA sequencing (Eurofins Genomics, Tokyo). In addition, the deletion was a frameshift that inhibited protein synthesis and it was confirmed that PAD2 protein was not expressed in PAD2KO mice (Fig. 1c). All mice were housed at 22 ± 1 °C under a 12 h light/dark cycle. This study was conducted in strict accordance with ARRIVE guidelines[28]. Experimental protocols, including animal euthanasia methods, were approved by the Experimental Animal Research Committee of Kyoto Pharmaceutical University (permit number: 19-007).

Induction of experimental colitis

Experimental colitis was established as previously described[27,29,30]. Colitis was induced by a single rectal injection with 0.1 ml of 2,4,6-trinitrobenzenesulfonic acid (TNBS; 80 mg kg^{-1} in 30% ethanol solution; Sigma-Aldrich, St. Louis, MO, USA) under anesthetic induced using three mixed agents (medetomidine hydrochloride, 0.75 mg kg^{-1}; midazolam, 4 mg kg^{-1}; butorphanol tartrate, 5 mg kg^{-1}). Control mice received 0.1 ml of a 30% ethanol solution. Body weight was measured daily, and other assessments were performed on day three, after colon removal from mice euthanized by cervical dislocation.

Macroscopic and histological analyses

Colons were ablated three days after TNBS or vehicle administration. The colons were then cut and opened, and the area of macroscopic damage was determined using ImageJ software 1.53e (NIH, Bethesda, MD, USA, https://imagej.net/). Colon tissues including the area of inflammation were fixed in 10% formalin, embedded in paraffin, cut into 4-μm sections, and stained with hematoxylin and eosin (H&E). Histological images were obtained using a fluorescence microscope (BZ-X810; KEYENCE, Osaka).

Detection of myeloperoxidase (MPO) activity

MPO activity was analyzed as described previously[31]. Colon tissues were homogenized in 50 mM phosphate buffer containing 0.5% hexadecyltrimethylammonium bromide (pH 6.0; Wako Pure Chemical Industries Ltd., Osaka). Homogenized samples were subjected to three freeze–thaw cycles and centrifuged at 1500 rpm for 10 min at 4 °C. The supernatant (5 μl) was diluted with 10 mM phosphate buffer (pH 6.0, 95 μl) and 1.5 mM o-dianisidine hydrochloride (50 μl; Sigma Aldrich) containing 0.0015% (w/v) hydrogen peroxide. Sequential absorbance changes at 450 nm were measured using a Multiskan Go spectrophotometer. MPO activity (U/mg protein) was calculated based on the amount of MPO present, which was estimated using a standard curve, and the protein content was determined using a Pierce BCA Protein Assay Kit (Thermo Fisher Scientific Inc., Waltham, MA, USA).

Isolation of intraperitoneal macrophages and neutrophils

Intraperitoneal macrophages and neutrophils were obtained from wild-type and PAD2KO mice injected intraperitoneally with 2 ml of 3% (w/v) thioglycolate (Nissui Pharmaceutical Co., Ltd., Tokyo). Three days or four hours after injection, macrophages or neutrophils infiltrating the peritoneal cavity were collected by intraperitoneal injection of PBS. The cells were then washed with PBS and used for each experiment.

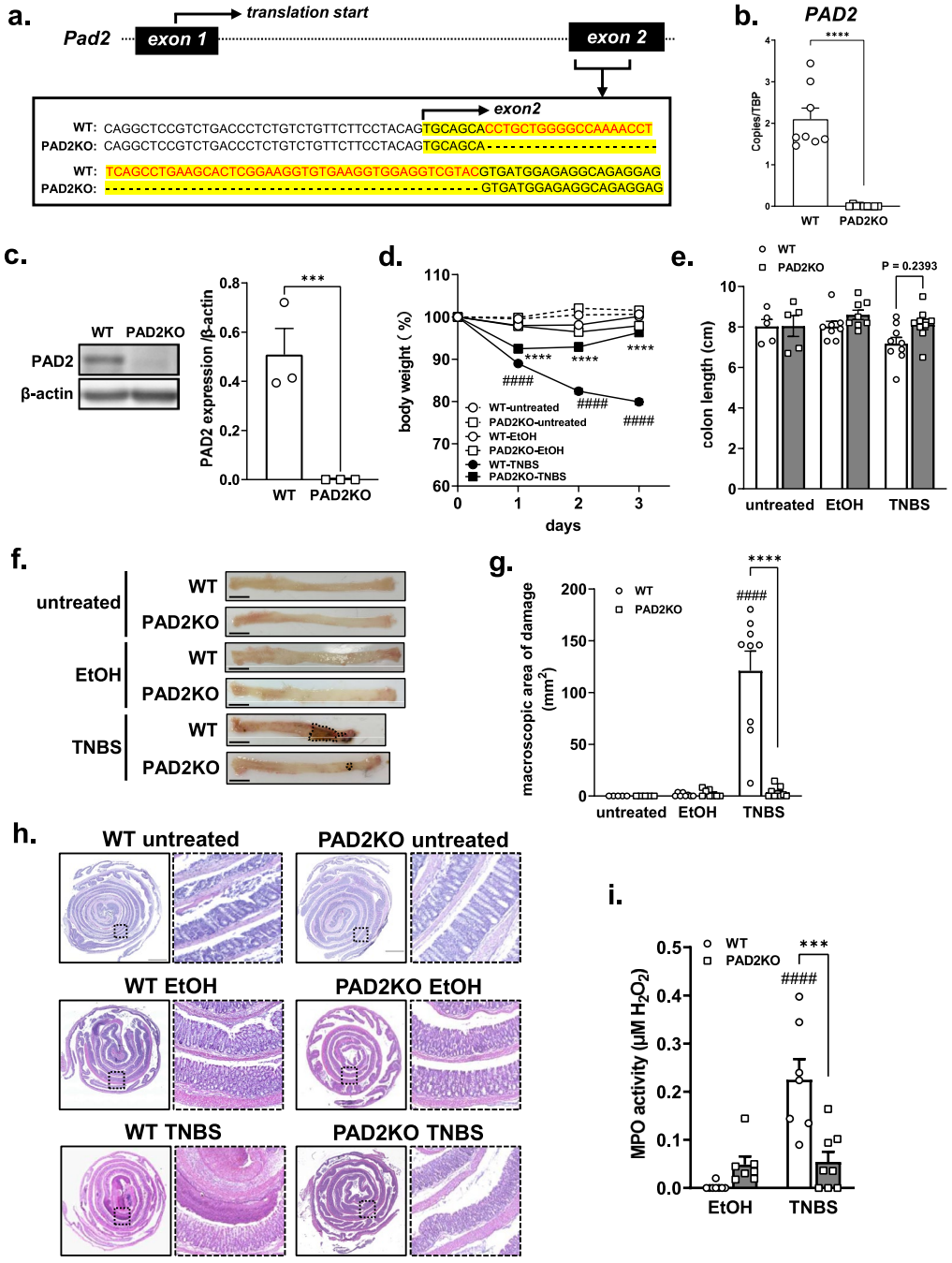

Fig. 1. Generation of PAD2KO mice using the CRISPR-Cas9 systems and pathogenesis of TNBS-induced colitis in wild-type and PAD2KO mice. (**a**) The sequences produced for the generation of PAD2KO mice using the CRISPR-Cas9 systems, deficient in 61-bp on exon2 of the genomic PAD2 DNA. (**b**) PAD2 mRNA level was determined in intraperitoneal macrophages by qRT-PCR normalized to TBP. Data were presented as the means ± S.E.M. (n = 8). ****P < 0.0001 vs. wild-type (WT) mice. (**c**) PAD2 expression was determined in intraperitoneal macrophages by western blotting normalized to β-actin expression. Data are presented as the means ± S.E.M. (n = 3). ***P < 0.001 vs. WT mice. (**d**) Body weight was measured daily in untreated-, vehicle (30% ethanol)-, or TNBS-injected WT and PAD2KO mice. On day 3, colon length was measured (**e**), representative images were obtained (**f**), and macroscopic analyses of the injured area were carried out using Image J (**g**). Scale bars are 10 mm. Histological changes were observed following H&E staining (**h**). (**i**) MPO activity was determined in those mice. Data are presented as the means ± S.E.M. (n = 8–9). ####P < 0.0001 vs. vehicle-injected mice (WT EtOH), and ****P < 0.0001, ***P < 0.001, *P < 0.05 vs. TNBS-injected mice (WT TNBS).

Quantitative reverse transcription polymerase chain reaction (qRT-PCR)

qRT-PCR was performed as previously described[30,32]. Total RNA was extracted from homogenized colonic tissues or intraperitoneal macrophages washed with PBS using Sepasol RNA I Super G (Nacalai Tesque, Kyoto), and reverse transcribed using PrimeScript RT Master Mix (Perfect Real Time) (Takara, Shiga). qRT-PCR was performed on a Thermal Cycler Dice Real-Time System (Takara) using TB Green Premix Ex Taq II (Tli RNaseH Plus) (Takara). The primer sets for TBP (MA050367), TNFα (MA097070), IL-1β (MA025939), IL-12 (MA025924), IL-23 (MA095159), IFNγ (MA025911), CXCL2 (MA152904), CD86 (MA197955), and CD206 (MA137874) were obtained from the Perfect Real-Time Supporting System (Takara), and PAD2 primer (Forward; 5′-GCACTCGGAAGGTGTGAAGG-3′, Reverse; 5′-AGTTGACAGTGACCTTGTCGC-3′), iNOS primer (Forward; 5′-GTCATGAGCAAAGGCGCAGA-3′, Reverse; 5′-GGAATGGAGACTGTCCCAGCA-3′), and arginase-1 (Arg-1) primer (Forward; 5′-GAAGAGTCAGTCTGGTGCTGG-3′, Reverse; 5′-CAGTGTGA GCATCCACCCAA-3′) was designed. The expression of each gene was calculated using the comparative ΔΔCt method.

Western blotting

Western blotting was performed as previously described[27]. Intraperitoneal macrophages were suspended in RIPA buffer (50 mM Tris–HCl, pH 7.6, containing 1 mM EDTA, 150 mM NaCl, 0.5% sodium deoxycholate, 0.1% sodium dodecyl sulfate (SDS), 1% Nonidet P-40, and a protease inhibitor cocktail), and a whole cell solution was collected after centrifugation at 13,200×*g* for 10 min. The protein concentration was determined by performing a BCA protein assay. The extracts were mixed with SDS sample buffer (62.5 mM Tris–HCl, pH 6.8, containing 2% SDS, 5% glycerol, 5% 2-mercaptoethanol, and 0.002% bromophenol blue), boiled for 5 min, and then separated using SDS-PAGE on 12% (w/v) polyacrylamide gels. The separated proteins were then electrophoretically transferred onto PVDF membranes, and nonspecific binding was blocked with 5% skim milk in PBS containing 0.1% Tween 20 (PBST). The membranes were then incubated with PAD2 antibody (1:500) (Proteintech, 12110-1-AP) and β-actin antibody (1:2000) (CST, #4970). After washing with PBST, the membranes were incubated with anti-rabbit IgG HRP-linked antibody (1:2,000; CST, #7074). The protein bands were detected using Western Lightning® Plus-ECL (PerkinElmer, Waltham, MA, USA) and imaged with a FUSION Solo 6S (Vilber, Lourmat, Marne-la-Vallée, France).

Immunofluorescence staining

Immunofluorescence staining was performed as previously described[16,27]. Colonic tissues were fixed in 4% paraformaldehyde for 2 h and cryoprotected in 20% sucrose solution overnight prior to embedding in an optimal cutting temperature compound (Sakura Finetek, Tokyo). Tissues were then sectioned at 20 μm thickness using a cryostat (Leica Instruments, Nussloch, Germany) and thaw-mounted onto Superfrost Plus slides (Matsunami, Osaka). Non-specific binding was blocked using 10% normal donkey serum (Millipore, Temecula, CA, USA) in PBS containing 0.1% sodium azide for 1 h at room temperature. Further, the cells to be evaluated for ETs including METs were resuspended in Dulbecco's modified Eagle's medium (DMEM; Nacalai Tesque, Kyoto) containing 10% fetal bovine serum (FBS), 100 U/ml penicillin and 100 μg/ml streptomycin and were immobilized on 8-well chamber slides (ibidi, Gräfelfing, Germany) coated with poly-lysine. After incubation on a slide with 10 μM A23187 and 1 mM $CaCl_2$ or 10 μM phorbol myristate acetate (PMA) for 4 h, the intraperitoneal macrophages or neutrophils were fixed in 4% paraformaldehyde for 20 min, washed with PBS, and blocked with 1% BSA (Nacalai) in PBS for 1 h at room temperature. These samples were then incubated overnight at room temperature with rabbit anti-citrullinated histone H3 (citH3; 1:500, Abcam, ab5103), goat anti-MPO (2 μg ml^{-1}, R&D, AF3667), or rat anti-F4/80 (1:1000, Bio-Rad, MCA497GA), respectively. The samples were then incubated with donkey anti-rabbit IgG (Alexa Fluor 594, 1:800; Thermo Fisher Scientific), donkey anti-goat IgG (Alexa Fluor 488, 1:800; Thermo Fisher Scientific), or donkey anti-rat IgG (Alexa Fluor 488, 1:1600; Thermo Fisher Scientific) secondary antibodies for 3 h at room temperature. After washing with PBS, Hoechst33258 was used to counterstain the nuclei, and images were obtained using a fluorescence microscope (BZ-X810; KEYENCE). The quantity of ETs or METs in the tissues was determined as the percentage of triple-positive citH3-MPO-Hoechst33258 or F4/80-citH3-Hoechst33258 signals in the area of the visible part of the tissue, and the quantity of NETs or METs in the neutrophils or macrophages was determined as the percentage of triple-positive citH3-MPO-Hoechst33258 signals among the total number of Hoechst33258-stained total cells in the visible region using ImageJ software 1.53e (NIH).

Flow cytometry

Intraperitoneal macrophages were obtained as described previously. The samples containing 2×10^6 cells were stained with dead cells by Zombie Aqua™ Fixable viability kit (BioLegend, San Diego, CA, USA) and blocked by Fc receptor CD16/CD32 in mice (BD Biosciences, Franklin Lakes, NJ, USA) for 15 min at room temperature. For detecting macrophage surface markers, the cells were incubated with APC anti-mouse/human CD11b, PerCP/Cyanine5.5 anti-mouse F4/80, PE/Cyanine7 anti-mouse CD80 and Brilliant Violet 421 anti-mouse CD163 antibody for 30 min at 4 ℃. Following incubation, all cells were washed with stain buffer (BD Biosciences) and the surface marker fluorescence was used to gate cells that were not stained as dead cells; M1 ($CD80^+$) or M2 macrophages ($CD163^+$) were then distinguished from the $CD11b^+$ and $F4/80^+$-positive population (whole macrophages). Flow cytometric measurements were performed using a BD LSRFortessa™ X-20 flow cytometer (BD Biosciences).

Statistical analyses

The data are presented as mean ± SEM. Statistical analyses were performed using the GraphPad Prism 9.4.0 (GraphPad Software, La Jolla, CA, USA, https://www.graphpad.com/). Multiple groups were compared using

two-way ANOVA, followed by a post-hoc Holm–Sidak test. Parametric data were tested using the Student's t-test. Statistical significance was set at P values < 0.05.

Results

Pathogenesis of TNBS-induced colitis model was ameliorated in PAD2KO mice

We previously reported the involvement of NETs induction through PAD4 activity in TNBS-induced colitis, and that treatment with Cl-amidine and DNase I attenuates the pathogenesis of TNBS-induced colitis[27]. Similarly, we investigated whether PAD2KO mice exhibited TNBS-induced pathogenesis compared to that in wild-type (WT) mice. We used the CRISPR/Cas9 system to delete bases encoding a part of exon 2 of the *PAD2* gene, as shown in Fig. 1a. To evaluate whether PAD2-deficient (PAD2KO) mice were generated by partial gene deletion, PAD2 mRNA and protein expression in macrophages were determined. Although PAD2 was expressed in intraperitoneal macrophages, PAD2 expression was not detected in PAD2KO mice (Fig. 1b and c). These results suggest that PAD2KO mice can be generated using the CRISPR-Cas9 system. As shown in Fig. 1d, body weight continued to decrease significantly for up to three days after TNBS administration (80 mg kg^{-1} in 30% ethanol). Body weight loss due to TNBS administration was recovered in PAD2KO mice (Fig. 1d). After TNBS administration for three days, colon length was measured (Fig. 1e), the development of ulceration was determined by macroscopic observation (Fig. 1f and g) and histological analysis (Fig. 1h), and MPO activity was measured (Fig. 1i). Although TNBS administration tended to reduce colon length (Fig. 1e), significantly induce ulcer development, and enhanced MPO activity in WT mice, these effects were significantly attenuated in PAD2KO mice (Fig. 1f–i). Colon length shortening tended to be suppressed in PAD2KO mice (Fig. 1e). These results suggest that PAD2 may be involved in the pathogenesis of TNBS-induced colitis.

PAD2KO mice showed attenuated inflammatory cytokine expression in TNBS-induced colitis

We investigated the mRNA expression of inflammatory cytokines, chemokines, and Th1/Th17-related cytokines in WT or PAD2KO mice with TNBS-induced colitis. After TNBS administration for three days, colon tissue showed significantly increased TNFα, IL-1β, IL-12, and CXCL2 mRNA expression in contrast with that in vehicle (30% ethanol)-administrated mice (Fig. 2a–c and f), while IL-23 and IFNγ expression tended to be increased in TNBS-induced colitis tissue (Fig. 2d and e). The upregulation of TNFα, IL-1β and CXCL2 in TNBS-induced colitis was significantly attenuated in PAD2KO mice, while IL-12, IL-23 and IFNγ expression tended to be attenuated in PAD2KO mice (Fig. 2c–e). PAD2 expression was not significantly altered in TNBS-treated mice and was not observed in PAD2KO mice (Fig. 2g). Overall, PAD2 deficiency may alleviate the pathology of TNBS-induced colitis by suppressing inflammatory cytokine expression.

PAD2KO mice showed reduced extracellular traps in TNBS-induced colitis

Extracellular traps (ETs) in neutrophils and macrophages were evaluated by co-immunostaining for MPO, citrullinated histone H3, and DNA in the colon tissues. METs were evaluated by co-immunostaining for F4/80, citrullinated histone H3, and DNA. As shown in Fig. 3a and b, ETs were significantly increased in the ulcerated portions of colon tissues in TNBS-administrated WT mice compared to those in vehicle-administrated mice. The ET induction by TNBS was attenuated in PAD2KO mice (Fig. 3a and b). Moreover, MET induction was similarly increased by TNBS administration and reduced in PAD2KO mice (Fig. 3c and d). These results indicate that ETs, including METs, are upregulated in TNBS-induced colitis, but suppressed in PAD2KO mice.

Intraperitoneal macrophages in PAD2KO mice did not suppress MET induction

To clarify whether the suppression of TNBS-induced ET and MET induction in PAD2KO mice was due to the direct involvement of PAD2, we isolated neutrophils or macrophages from PAD2KO mice and demonstrated the induction of NETs and METs. NETs and METs are known to be induced by calcium ionophores such as A23187 or phorbol myristate acetate (PMA)[11,23]. Our previous results showed that NETs were induced by PAD4 activity[27]. We therefore investigated whether ETs were induced by A23187 and PMA in intraperitoneal macrophages and neutrophils, and whether PAD2KO mice-derived macrophages and neutrophils suppressed MET and NET induction, respectively. Intraperitoneal macrophages and neutrophils were isolated from wild-type and PAD2KO mice injected intraperitoneally with 3% thioglycolate (TGC) for three days or four hours, respectively. As shown in Fig. 4a, the release of DNA in MET induction upon treatment with 10 μM A23187 and 10 μM PMA was confirmed using SYTOX green. Furthermore, MET and NET induction was confirmed by co-immunostaining for MPO, citrullinated histone H3, and DNA; however, MET or NET induction was not suppressed in macrophages or neutrophils derived from PAD2KO mice (Fig. 4b–e). These results suggest that PAD2 may not be involved in ET induction and that the suppression of TNBS-induced colitis pathogenesis in PAD2KO mice may involve other mechanisms.

PAD2 deficiency in macrophage altered macrophage differentiation and suppressed inflammatory cytokine expression

Since it was suggested that PAD2 is not involved in MET induction, we investigated other PAD2-related factors that might contribute to pathogenesis of IBD. It is known that macrophage polarization and induction of Th1/17-related cytokines are involved in IBD[33,34], and that inflammatory cytokines and chemokines induce ETs[35,36]. Macrophages that infiltrated into the peritoneal cavity by treatment with 3% TGC were slightly activated, as shown in Fig. 5; most macrophages were M1 macrophages and untreated macrophages showed high expression of inflammatory cytokines, Th1/Th17-related cytokines, and chemokines. Interestingly, M1 macrophages were significantly decreased while M2 macrophages tended to be increased among intraperitoneal macrophages derived from PAD2KO mice (Fig. 5a and b). Moreover, the expression of M1 macrophage-related genes, such as CD86 and iNOS, was significantly decreased while the expression of M2 macrophage-related genes, such as

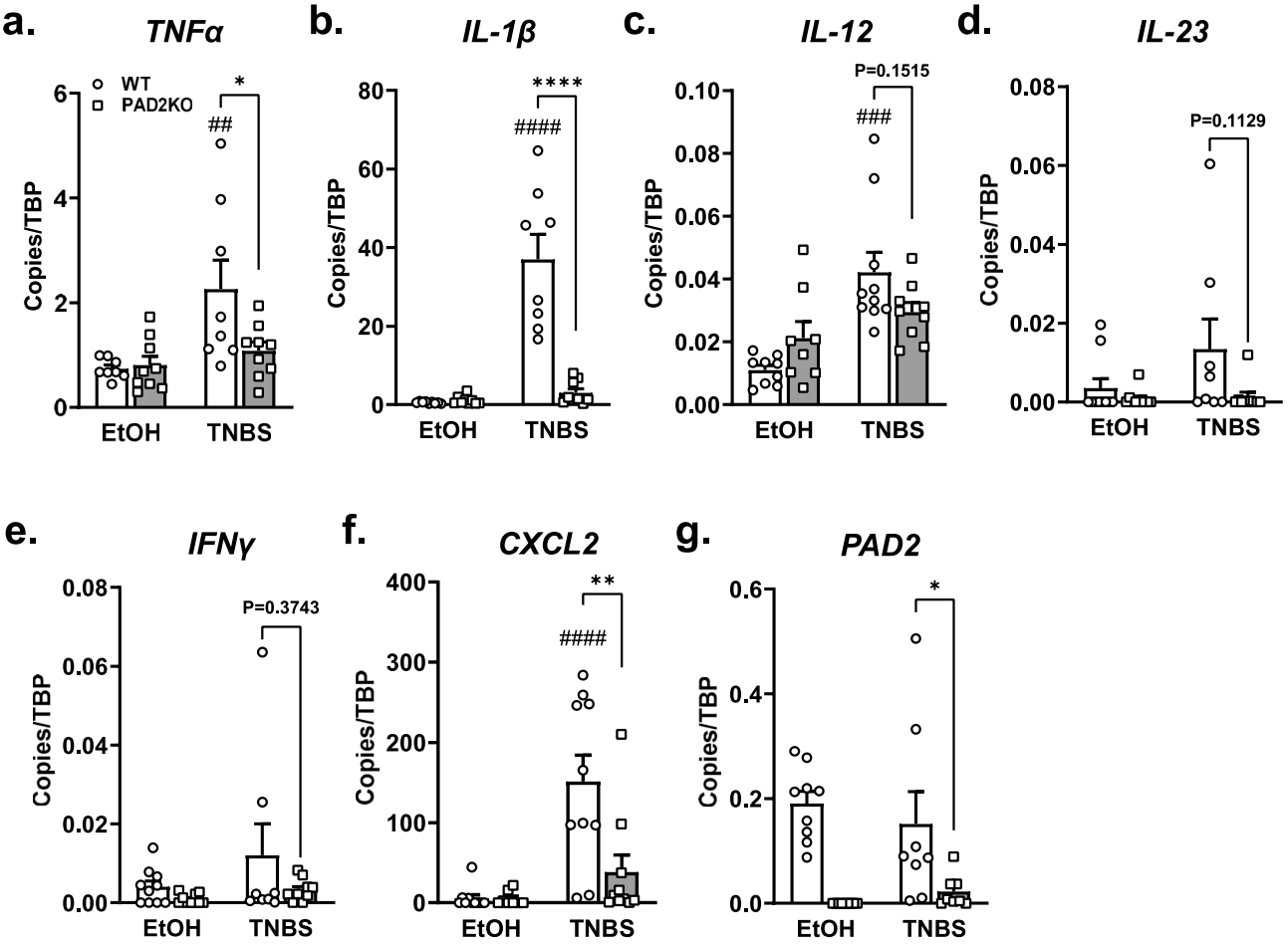

Fig. 2. Expression of inflammatory cytokines, chemokines, and PAD2 in PAD2KO mice. (**a**) TNFα, (**b**) IL-1β, (**c**) IL-12, (**d**) IL-23, (**e**) IFNγ, (**f**) CXCL2, and (**g**) PAD2 mRNA expression were determined using qRT-PCR in colon tissues of vehicle (30% ethanol)-, or TNBS-injected WT and PAD2KO mice on day 3, and mRNA levels were normalized to TBP. Data are presented as the means ± S.E.M. (n = 8–10). $^{\#\#\#\#}P < 0.0001$, $^{\#\#\#}P < 0.001$, $^{\#\#}P < 0.01$ vs. vehicle-injected mice (WT EtOH), and $^{****}P < 0.0001$, $^{*}P < 0.05$ vs. TNBS-injected mice (WT TNBS).

CD206, was significantly increased, although arginase-1 expression was unchanged (Fig. 5c–f). Furthermore, the upregulation of TNFα, IL-1β, IL-12, IL-23 and CXCL2 mRNA expression was decreased in PAD2KO mouse-derived macrophages (Fig. 5g–k). Taken together, PAD2 deficiency in macrophages may decrease the number of M1 macrophages, which in turn reduces the expression of inflammatory cytokines and chemokines.

Discussion

ETs are involved in several inflammatory diseases, and citrullination of histones is an important factor in the induction of ETs. In this study, we investigated the role of PAD2, a key enzyme in citrullination, and its involvement in ET formation in IBD, using a TNBS-induced murine colitis model. To clarify the importance of PAD2 in the immune responses in this colitis model, we generated PAD2KO mice. Our results demonstrated alleviated pathogenesis of TNBS-induced colitis in PAD2KO mice through suppression of immune responses, particularly macrophage activity.

Activated neutrophils and macrophages are known to infiltrate the intestinal mucosa in IBD, including ulcerative colitis and Crohn's disease, and neutrophils are known to induce NETs[37]. NETs exert antibacterial effects and are induced in various chronic inflammatory diseases; they are thus believed to be involved in inflammatory signaling pathways including immune responses. NET induction contributes to IBD pathogenesis by impairing the intestinal epithelial barrier[8], and induce thrombus formation with IBD[21]. Accordingly, NETs may also play a role in the pathogenesis and secondary effects of IBD. We previously reported that NETs mediated by PAD4 activity were involved in the pathogenesis of experimental colitis[27]. In the present study, we observed that NETs as well as METs were induced in TNBS-induced colitis, suggesting that macrophages also induce ETs in the excessive immune response in the intestinal environment, such as IBD. Additionally, as METs are similar to the DNA released by NET induction[38], treatment with DNase I, known to be a NETs inhibitor and suppressed in experimental colitis[8,27], may also ameliorate colitis by inhibiting METs in this colitis model.

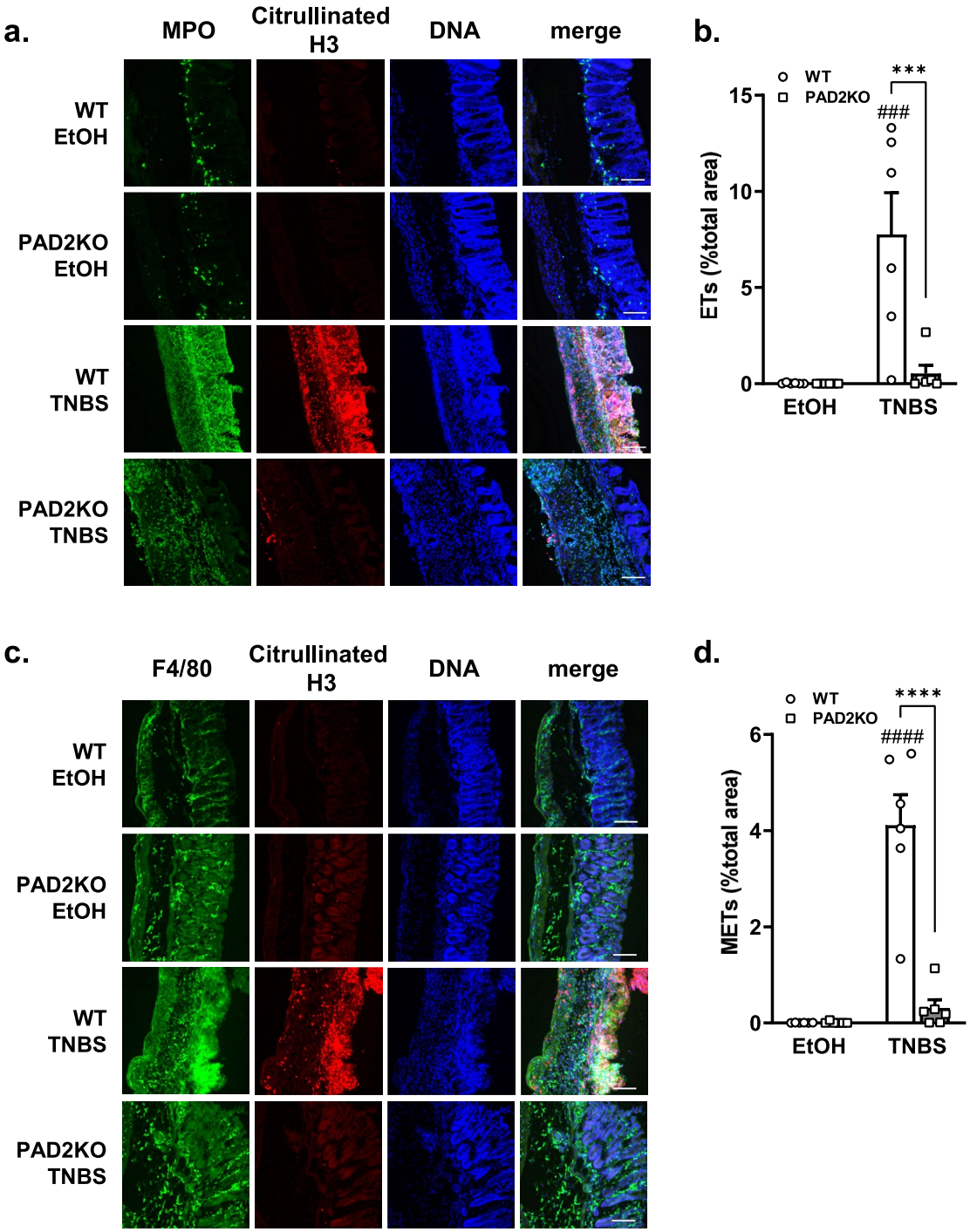

Fig. 3. ETs and METs induction in TNBS-induced colitis in PAD2KO mice. (**a**) Extracellular traps (ETs) were evaluated by immunohistological co-staining with anti-myeloperoxidase (MPO; green), anti-citrullinated histone H3 (Citrullinated H3; red), and Hoechst33258 (DNA; blue) in colon tissues of vehicle (30% ethanol)-, or TNBS-injected WT and PAD2KO mice. (**c**) Macrophage extracellular traps (METs) were evaluated by immunohistological co-staining with anti-F4/80 (F4/80; green), anti-citrullinated histone H3 (Citrullinated H3; red), and Hoechst33258 (DNA; blue) in colon tissues of vehicle (30% ethanol)-, or TNBS-injected WT and PAD2KO mice. The quantity of ETs (**b**) and METs (**d**) were determined as the area of MPO-positive, Citrullinated H3-positive, and DNA-positive sites (ETs) or F4/80-positive, Citrullinated H3-positive, and DNA-positive sites (METs) per colon tissue area in the image, respectively. Data are presented as the means ± S.E.M. (n = 6). $^{\#\#\#\#}P < 0.0001$, $^{\#\#\#}P < 0.001$ vs. vehicle-injected mice (WT EtOH), and $^{****}P < 0.0001$, $^{***}P < 0.001$ vs. TNBS-injected mice (WT TNBS).

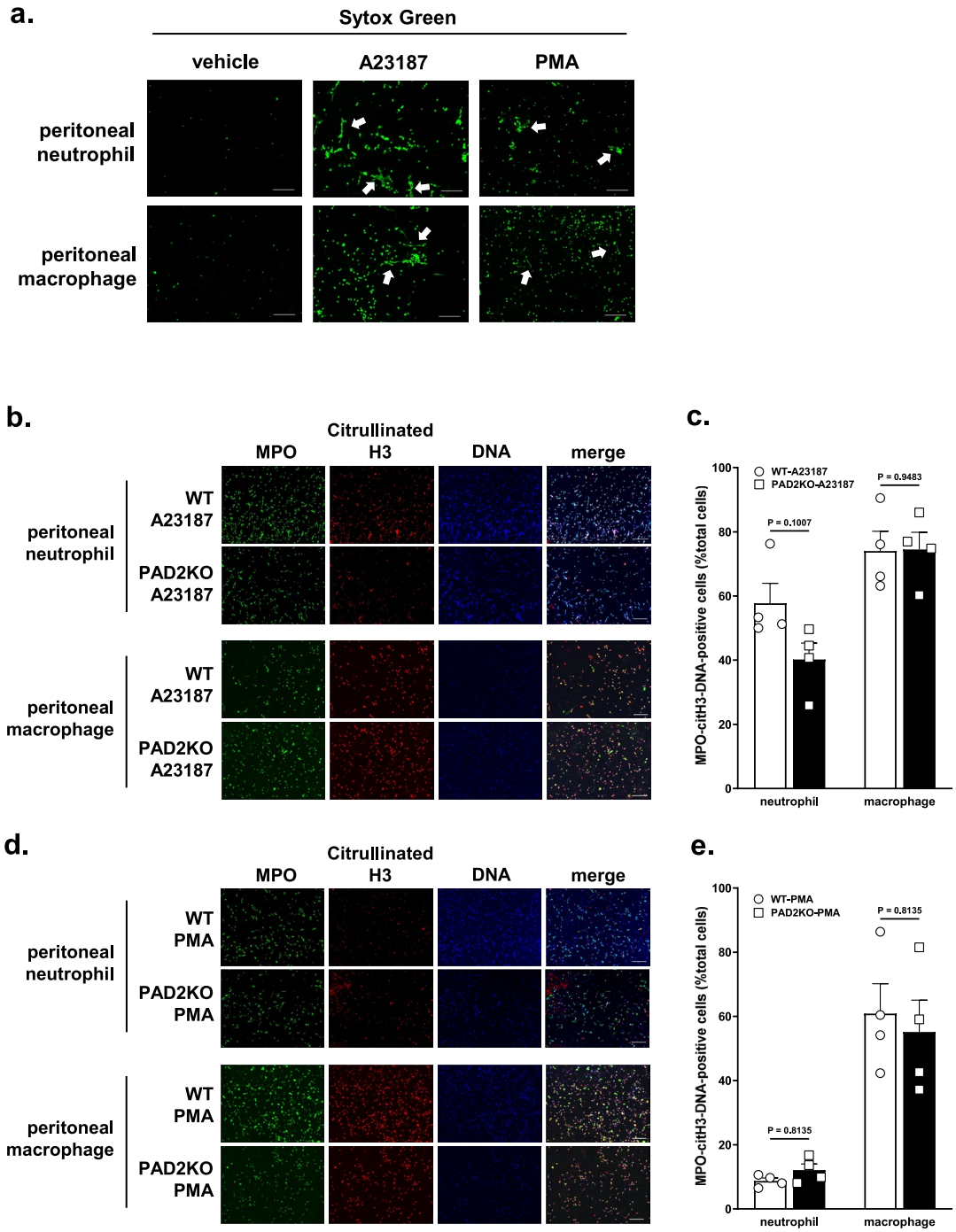

Fig. 4. Evaluation of NETs and METs in intraperitoneal macrophages from WT and PAD2KO mice. NETs and METs are induced by treatment with 10 μM A23187 (Ca ionophore) and 10 μM PMA (phorbol 12-myristate 13-acetate) for 4 h in intraperitoneal neutrophils and macrophages derived from WT mice. (**a**) Extracellular DNA was stained using SYTOX Green. (**b**–**d**) NETs and METs induced in neutrophils and macrophages derived from WT mice or PAD2KO mice were evaluated by immunofluorescence co-staining with anti-myeloperoxidase (MPO; green), anti-citrullinated histone H3 (Citrullinated H3; red), and Hoechst33258 (DNA; blue). Scale bar is 200 μm. Data are presented as the means ± S.E.M. (n = 4).

PAD2 is widely distributed in mammals and is expressed in hematopoietic cells such as macrophages and T cells[25,39], as well as in the central nervous system[40,41], spleen[42], and liver[43]. Some studies have demonstrated that PAD2-mediated citrullination contributes to the differentiation of oligodendrocytes and T cells[44,45], fibrosis[43], and secretion of IgM and IgA by citrullinated MZB1 in B cells[46]. Moreover, MET induction requires PAD2 and is suppressed by PAD2 inhibitors[19,26]. However, in this study, ET induction was not decreased in PAD2KO-derived macrophages and neutrophils. TNBS may induce ROS[47], and the treatment with PMA is known to

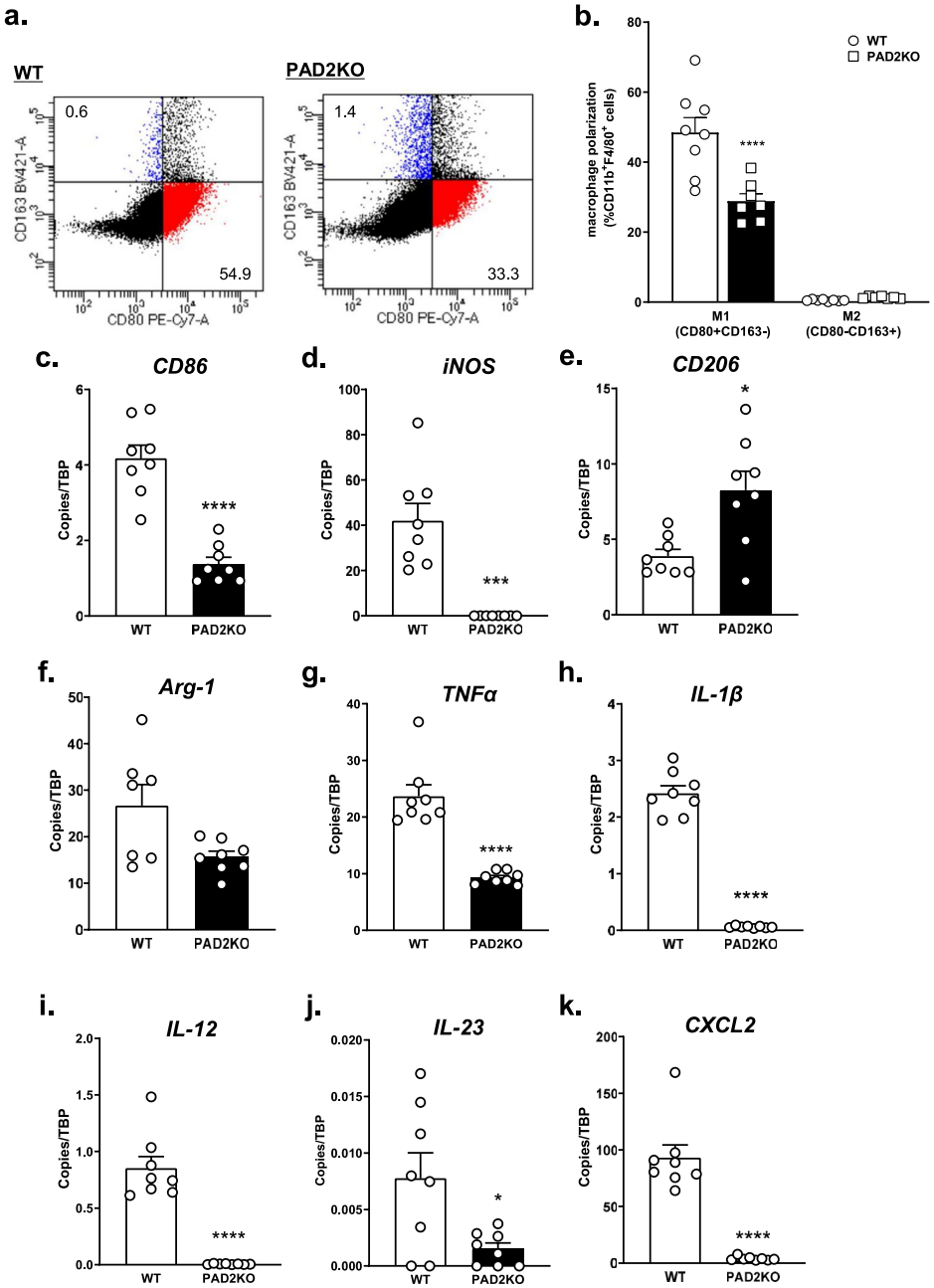

Fig. 5. Macrophage polarization and inflammatory mediator expression in intraperitoneal macrophages derived from PAD2KO mice. (**a**,**b**) Macrophage polarization was determined using flow cytometry. CD11b-positive and F4/80-positive cells were sorted from the live cells in the population of intraperitoneal macrophages, and M1 and M2 macrophages were then determined by CD80-positive cells (M1) or CD163-positive cells (M2) from the sorted population. (**c**) CD86, (**d**) iNOS, (**e**) CD206, (**f**) arginiase-1 (Arg-1), (**g**) TNFα, (**h**) IL-1β, (**i**) IL-12, (**j**) IL-23, and (**k**) CXCL2 mRNA expression were determined using qRT-PCR in unstimulated intraperitoneal macrophages from WT and PAD2KO mice, and mRNA levels were normalized to TBP. Data are presented as the means ± S.E.M. (n = 7–8). ****P < 0.0001, **P < 0.01 vs. WT macrophages.

induce NADPH oxidase (NOX)-dependent ETs, which involves ROS[14,23]. Therefore, PAD2 may not be involved in the induction of NOX-dependent METs and NETs similar to TNBS treatment. Additionally, PMA-induced ETs were less induced in neutrophils than in macrophages in mice. It has been previously reported that PMA-induced NETs are difficult to induce in neutrophils in mice[48]. In contrast, PMA-induced METs were induced early, suggesting that the NOX-dependent pathway is important in METs. ET induction is a stepwise process, and the key events may be chromatin decondensation[11], nuclear envelope rupture[49], and subsequent plasma membrane breakdown[50]. In particular, the importance in chromatin decondensation of PAD4 as a key factor in NET formation is understood because the inhibition of PAD4 activity results in an inability to induce NETs, and the nuclear localization of PAD4 clearly explains its involvement in histone citrullination. Although PAD2

has also been reported to be involved in the induction of ETs[26], it is unlikely that PAD2 citrullinates histones because it does not directly translocate into the nuclear. Further, PAD4 is expressed in macrophages and METs are induced by PAD4 activity[26,51]. PAD4 activity may have been involved in MET induction in this study, but the details remain unclear. Overall, citrullination of PAD2 is not essential for MET induction, and other factors such as PAD4 or NOX activity may be involved in the induction of METs.

TNBS-induced colitis is an established CD-like colitis model with activation of Th1/Th17-immune responses[52]. In our previous study, the expression of inflammatory cytokines, Th1/Th17-related cytokines, and chemokines, such as TNFα, IL-1β, IFNγ, IL-12, IL-23 and CXCL2 were found to be increased in TNBS-induced colitis tissue[27,30]. In this study, we showed that the upregulation of these cytokines in TNBS-induced colitis was prevented in PAD2KO mice. Furthermore, PAD2 is reported to control the differentiation of naïve Th cells into Th17 by citrullinating the transcription factor RoryT[45], suggesting that PAD2 can mediated the pathogenesis of TNBS-induced colitis by regulating inflammatory cytokines and chemokines, as well as Th1/Th17-immune responses.

Macrophage polarization plays important roles in IBD through maintaining homeostasis of intestinal immunity[33]. M1 macrophages release various inflammatory cytokines, such as TNFα, IL-1β, IL-12, and IL-23, whereas M2 macrophages release anti-inflammatory cytokines, such as IL-10. The inflammatory cytokines released by M1 macrophages exacerbate IBD, whereas M2 macrophages can suppress upregulated inflammation and repair intestinal epithelial tissue injury associated with IBD pathogenesis[33,53]. Our results demonstrated that most peritoneal macrophages were M1 macrophages and that inflammatory cytokines were increased; however, PAD2KO mice-derived peritoneal macrophages showed significantly decreased M1 macrophages and reduced inflammatory cytokines expression. As TNFα, IL-1β, IL-12, and IL-23 released from M1 macrophages are involved in Th1/Th17-immune responses and inflammatory cytokines and CXCL2 is involved in ET induction[30,33,36], the increased expression of various cytokines and ET induction observed in TNBS-induced colitis may be attributed to the role of PAD2 in macrophages. Moreover, M2 macrophages tended to be enhanced by PAD2 deficiency in this study. Stachowicz et al. also showed that PAD2 modulated the M2 phenotype in THP-1 macrophage[54]. Nuclear translocation of NF-kB is an important factor in inflammatory responses including TLR4 signaling; interestingly, the nuclear translocation of NF-kB p65 is suppressed by inhibiting citrullination[55]. Therefore, PAD2 is involved in the regulation of macrophage polarization, and PAD2 deficiency may suppress M1 differentiation and reduce the expression of inflammatory cytokines in immune responses, contributing to the amelioration of pathogenesis in TNBS-induced colitis. However, the proteins citrullinated by PAD2 and their involvement in macrophage polarization remain unclear. Further studies are thus required to elucidate the mechanisms underlying M1 and M2 macrophage differentiation induced by citrullination with PAD2 activity.

In conclusion, we demonstrated that the pathogenesis of TNBS-induced colitis in mice was ameliorated by PAD2 inhibition. In this case, MET induction was suppressed along with the amelioration of pathogenesis. PAD2 inhibition did not directly suppress MET induction, but rather reduced the expression of inflammatory cytokines, including Th1/Th17-related cytokines, by controlling the M1/M2 differentiation of macrophages. Overall, this study clarifies part of the pathogenic mechanisms of IBD and demonstrates the importance of macrophage function via citrullination by PAD2 activity through a mechanism other than ET induction. Furthermore, we believe that the citrullination of proteins mediated by PAD4, which is involved in the ET-dependent pathway, and PAD2, which is involved in the ET-independent pathway, will lead to new IBD therapeutic strategies in the future.

Data availability

All data supporting the findings during this study are included in this published article. The authors will provide details upon request (request to: Corresponding author, Hiroyuki Yasuda).

Received: 24 June 2025; Accepted: 13 October 2025
Published online: 18 November 2025

References

1. Chen, Y., Cui, W., Li, X. & Yang, H. Interaction between commensal bacteria, immune response and the intestinal barrier in inflammatory bowel diseases. *Front. Immunol.* **12**, 761981. https://doi.org/10.3389/fimmu.2021.761981 (2021).
2. Kinchen, J. et al. Structural remodeling of the human colonic mesenchyme in inflammatory bowel disease. *Cell* **175**, 372–386. https://doi.org/10.1016/j.cell.2018.08.067 (2018).
3. Randhawa, P. K., Singh, K., Singh, N. & Jaggi, A. S. A review on chemical-induced inflammatory bowel disease models in rodents. *Korean J. Physiol. Pharmacol.* **18**, 279–288. https://doi.org/10.4196/kjpp.2014.18.4.279 (2014).
4. Kayama, H. & Takeda, K. Regulation of intestinal homeostasis by innate and adaptive immunity. *Int. Immunol.* **24**, 673–680. https://doi.org/10.1093/intimm/dxs094 (2012).
5. Brazil, J. C., Louis, N. A. & Parkos, C. A. The role of polymorphonuclear leukocyte trafficking in the perpetuation of inflammation during inflammatory bowel disease. *Inflamm. Bowel Dis.* **19**, 1556–1565. https://doi.org/10.1097/MIB.0b013e318281f54e (2013).
6. Garrido-Trigo, A. et al. Macrophage and neutrophil heterogeneity at single-cell spatial resolution in human inflammatory bowel disease. *Nat. Commun.* **14**, 4506. https://doi.org/10.1038/s41467-023-40156-6 (2023).
7. Zenewicz, L. A., Antov, A. & Flavell, R. A. CD4 T-cell differentiation and inflammatory bowel disease. *Trends. Mol. Med.* **15**, 199–207. https://doi.org/10.1016/j.molmed.2009.03.002 (2009).
8. Lin, E. Y. et al. Neutrophil extracellular traps impair intestinal barrier function during experimental colitis. *Biomedicines* **8**, 275. https://doi.org/10.3390/biomedicines8080275 (2020).
9. Chen, X. et al. Inhibition of HMGB1 improves experimental mice colitis by mediation NETs and macrophage polarization. *Cytokine* **176**, 156537. https://doi.org/10.1016/j.cyto.2024.156537 (2024).
10. Kessenbrock, K. et al. Netting neutrophils in autoimmune small-vessel vasculitis. *Nat. Med.* **15**, 623–625. https://doi.org/10.1038/nm.1959 (2009).
11. Wang, Y. et al. Histone hypercitrullination mediates chromatin decondensation and neutrophil extracellular trap formation. *J. Cell Biol.* **184**, 205–213. https://doi.org/10.1083/jcb.200806072 (2009).

12. Rasmussen, K. H. & Hawkins, C. L. Role of macrophage extracellular traps in innate immunity and inflammatory disease. *Biochem. Soc. Trans.* **50**, 21–32. https://doi.org/10.1042/BST20210962 (2022).
13. Mistry, P. et al. Transcriptomic, epigenetic, and functional analyses implicate neutrophil diversity in the pathogenesis of systemic lupus erythematosus. *Proc. Natl. Acad. Sci. USA* **116**, 25111–25228. https://doi.org/10.1073/pnas.1908576116 (2019).
14. Wright, H. L., Lyon, M., Chapman, E. A., Moots, R. J. & Edwards, S. W. Rheumatoid arthritis synovial fluid neutrophils drive inflammation through production of chemokines, reactive oxygen species, and neutrophil extracellular traps. *Front. Immunol.* **11**, 584116. https://doi.org/10.3389/fimmu.2020.584116 (2021).
15. Juha, M., Molnár, A., Jakus, Z. & Ledó, N. NETosis: an emerging therapeutic target in renal diseases. *Front. Immunol.* **14**, 1253667. https://doi.org/10.3389/fimmu.2023.1253667 (2023).
16. Yang, L. et al. DNA of neutrophil extracellular traps promotes cancer metastasis via CCDC25. *Nature* **583**, 133–138. https://doi.org/10.1038/s41586-020-2394-6 (2020).
17. Chen, Z. et al. Review: the emerging role of neutrophil extracellular traps in sepsis and sepsis-associated thrombosis. *Front. Cell Infect. Microbiol.* **11**, 653228. https://doi.org/10.3389/fcimb.2021.653228 (2021).
18. Wong, K. W. & Jacobs, W. R. Jr. Mycobacterium tuberculosis exploits human interferon gamma to stimulate macrophage extracellular trap formation and necrosis. *J. Infect. Dis.* **208**, 109–119. https://doi.org/10.1093/infdis/jit097 (2013).
19. Chen, T. et al. Interaction between macrophage extracellular traps and colon cancer cells promotes colon cancer invasion and correlates with unfavorable prognosis. *Front. Immunol.* **12**, 779325. https://doi.org/10.3389/fimmu.2021.779325 (2021).
20. Okubo, K. et al. Macrophage extracellular trap formation promoted by platelet activation is a key mediator of rhabdomyolysis-induced acute kidney injury. *Nat. Med.* **24**, 232–238. https://doi.org/10.1038/nm.4462 (2018).
21. Klopf, J., Brostjan, C., Eilenberg, W. & Neumayer, C. Neutrophil extracellular traps and their implications in cardiovascular and inflammatory disease. *Int. J. Mol. Sci.* **22**, 559. https://doi.org/10.3390/ijms22020559 (2021).
22. Zhai, M. et al. Extracellular traps from activated vascular smooth muscle cells drive the progression of atherosclerosis. *Nat. Commun.* **13**, 7500. https://doi.org/10.1038/s41467-022-35330-1 (2022).
23. Kirchner, T. et al. The impact of various reactive oxygen species on the formation of neutrophil extracellular traps. *Mediators Inflam.* **2012**, 849136. https://doi.org/10.1155/2012/849136 (2012).
24. Li, P. et al. PAD4 is essential for antibacterial innate immunity mediated by neutrophil extracellular traps. *J. Exp. Med.* **207**, 1853–1862. https://doi.org/10.1084/jem.20100239 (2010).
25. Vossenaar, E. R. et al. Expression and activity of citrullinating peptidylarginine deiminase enzymes in monocytes and macrophages. *Ann. Rheum. Dis.* **63**, 373–381. https://doi.org/10.1136/ard.2003.012211 (2004).
26. Bashar, S. J., Holmes, C. L. & Shelef, M. A. Macrophage extracellular traps require peptidylarginine deiminase 2 and 4 and are a source of citrullinated antigens bound by rheumatoid arthritis autoantibodies. *Front. Immunol.* **15**, 1167362. https://doi.org/10.3389/fimmu.2024.1167362 (2024).
27. Yasuda, H. et al. Neutrophil extracellular trap induction through peptidylarginine deiminase 4 activity is involved in 2,4,6-trinitrobenzenesulfonic acid-induced colitis. *Naunyn. Schmiedebergs. Arch. Pharmacol.* **397**, 3127–3140. https://doi.org/10.1007/s00210-023-02800-2 (2024).
28. ARRIVE guidelines; Experimental animals. https://arriveguidelines.org/arrive-guidelines/experimental-animals/8a/explanation.
29. Yokota, H. et al. NOX1/NADPH oxidase expressed in colonic macrophages contributes to the pathogenesis of colonic inflammation in trinitrobenzene sulfonic acid-induced murine colitis. *J. Pharmacol. Exp. Ther.* **360**, 192–200. https://doi.org/10.1124/jpet.116.235580 (2017).
30. Nakamoto, T., Matsumoto, K., Yasuda, H., Mori, Y. & Kato, S. Transient receptor potential melastatin 2 is involved in trinitrobenzene sulfonic acid-induced acute and chronic colitis-associated fibrosis progression in mice. *J. Pharmacol. Sci.* **154**, 18–29. https://doi.org/10.1016/j.jphs.2023.11.004 (2024).
31. Tsukahara, T. et al. G protein-coupled receptor 35 contributes to mucosal repair in mice via migration of colonic epithelial cells. *Pharmacol. Res.* **123**, 27–39. https://doi.org/10.1016/j.phrs.2017.06.009 (2017).
32. Utsumi, D., Matsumoto, K., Amagase, K., Horie, S. & Kato, S. 5-HT3 receptors promote colonic inflammation via activation of substance P/neurokinin-1 receptors in dextran sulphate sodium-induced murine colitis. *Br. J. Pharmacol.* **173**, 1835–1849. https://doi.org/10.1111/bph.13482 (2016).
33. Zhou, X. et al. YAP aggravates inflammatory bowel disease by regulating M1/M2 macrophage polarization and gut microbial homeostasis. *Cell Rep.* **27**, 1176–1189. https://doi.org/10.1016/j.celrep.2019.03.028 (2019).
34. Ryzhakov, G. et al. Alpha kinase 1 controls intestinal inflammation by suppressing the IL-12/Th1 axis. *Nat. Commun.* **9**, 3797. https://doi.org/10.1038/s41467-018-06085-5 (2018).
35. Dinallo, V. et al. Neutrophil extracellular traps sustain inflammatory signals in ulcerative colitis. *J. Crohns Colitis* **13**, 772–784. https://doi.org/10.1093/ecco-jcc/jjy215 (2019).
36. Wang, T. et al. Secreted protease PRSS35 suppresses hepatocellular carcinoma by disabling CXCL2-mediated neutrophil extracellular traps. *Nat. Commun.* **14**, 1513. https://doi.org/10.1038/s41467-023-37227-z (2023).
37. Maloy, K. J. & Powrie, F. Intestinal homeostasis and its breakdown in inflammatory bowel disease. *Nature* **474**, 298–306. https://doi.org/10.1038/nature10208 (2011).
38. Liu, P. et al. Escherichia coli and Candida albicans induced macrophage extracellular trap-like structures with limited microbicidal activity. *PLoS ONE* **9**, e90042. https://doi.org/10.1371/journal.pone.0090042 (2014).
39. Mergaert, A. M. et al. Peptidylarginine deiminase 2 in murine antiviral and autoimmune antibody responses. *J. Immunol. Res.* **2022**, 5258221. https://doi.org/10.1155/2022/5258221 (2022).
40. Kim, Y. et al. Peptidylarginine deiminase 2 autoantibodies are linked to less severe disease in multiple sclerosis and post-treatment lyme disease. *Front. Neurol.* **13**, 874211. https://doi.org/10.3389/fneur.2022.874211 (2022).
41. Yusuf, I. O. et al. PAD2 dysregulation and aberrant protein citrullination feature prominently in reactive astrogliosis and myelin protein aggregation in sporadic ALS. *Neurobiol. Dis.* **192**, 106414. https://doi.org/10.1016/j.nbd.2024.106414 (2024).
42. Van Beers, J. J., Zendman, A. J., Raijmakers, R., Stammen-Vogelzangs, J. & Pruijn, G. J. Peptidylarginine deiminase expression and activity in PAD2 knock-out and PAD4-low mice. *Biochimie* **95**, 299–308. https://doi.org/10.1016/j.biochi.2012.09.029 (2013).
43. Kim, S. E. et al. Accumulation of citrullinated glial fibrillary acidic protein in a mouse model of bile duct ligation-induced hepatic fibrosis. *PLoS ONE* **13**, e0201744. https://doi.org/10.1371/journal.pone.0201744 (2018).
44. Falcão, A. M. et al. PAD2-mediated citrullination contributes to efficient oligodendrocyte differentiation and myelination. *Cell Rep.* **27**, 1090-1102.e10. https://doi.org/10.1016/j.celrep.2019.03.108 (2019).
45. Sun, B. et al. Reciprocal regulation of Th2 and Th17 cells by PAD2-mediated citrullination. *JCI Insight* **4**, e129687. https://doi.org/10.1172/jci.insight.129687 (2019).
46. Geary, B. et al. Peptidylarginine deiminase 2 citrullinates MZB1 and promotes the secretion of IgM and IgA. *Front. Immunol.* **14**, 1290585. https://doi.org/10.3389/fimmu.2023.1290585 (2023).
47. Sui, Y. et al. Gut bacteria exacerbates TNBS-induced colitis and kidney injury through oxidative stress. *Redox Biol.* **72**, 103140. https://doi.org/10.1016/j.redox.2024.103140 (2024).
48. Yotsumoto, S. et al. Hyperoxidation of ether-linked phospholipids accelerates neutrophil extracellular trap formation. *Sci. Rep.* **7**, 16026. https://doi.org/10.1038/s41598-017-15668-z (2017).
49. Li, Y. et al. Nuclear envelope rupture and NET formation is driven by PKCα-mediated lamin B disassembly. *EMBO Rep.* **21**, e48779. https://doi.org/10.15252/embr.201948779 (2020).

50. Thiam, H. R. et al. NETosis proceeds by cytoskeleton and endomembrane disassembly and PAD4-mediated chromatin decondensation and nuclear envelope rupture. *Proc. Natl. Acad. Sci. USA* **117**, 7326–7337. https://doi.org/10.1073/pnas.1909546117 (2020).
51. Shen, Y. et al. Role of peptidyl arginine deiminase 4-dependent macrophage extracellular trap formation in type 1 diabetes pathogenesis. *Diabetes* **73**, 1862–1874. https://doi.org/10.2337/db23-1000 (2024).
52. Alex, P. et al. Distinct cytokine patterns identified from multiplex profiles of murine DSS and TNBS-induced colitis. *Inflamm. Bowel Dis.* **15**, 341–352. https://doi.org/10.1002/ibd.20753 (2009).
53. Lin, Y. et al. Chemerin aggravates DSS-induced colitis by suppressing M2 macrophage polarization. *Cell Mol. Immunol.* **11**, 355–366. https://doi.org/10.1038/cmi.2014.15 (2014).
54. Stachowicz, A. et al. Protein arginine deiminase 2 (PAD2) modulates the polarization of THP-1 macrophage to the anti-inflammatory M2 phenotype. *J. Inflamm.* **19**, 20. https://doi.org/10.1186/s12950-022-00317-8 (2022).
55. Sun, B. et al. Citrullination of NF-kappaB p65 promotes its nuclear localization and TLR-induced expression of IL-1beta and TNFalpha. *Sci. Immunol.* **2**, eaal3062. https://doi.org/10.1126/sciimmunol.aal3062 (2017).

Author contributions

Hiroyuki Yasuda: Conceptualization, Methodology, Investigation, Writing—Original Draft. Michiko Saito: Resources. Shusaku Hayashi: Methodology, Writing—Review, and Editing. Shinichi Kato: Conceptualization, Methodology, Writing—Review, and Editing.

Funding

This work was supported in part by Grants-in-Aid for Research from Kyoto Pharmaceutical University and JSPS KAKENHI (grant number JP21K15276 and JP25K10008).

Declarations

Ethics statement animal experimentation

This study was conducted in strict accordance with ARRIVE guidelines[28]. Experimental protocols, including animal euthanasia methods, were approved by the Experimental Animal Research Committee of Kyoto Pharmaceutical University (permit number: 19-007) and all methods were performed in accordance with the relevant guidelines and regulation.

Competing interests

The authors declare no competing interests.

Additional information

Correspondence and requests for materials should be addressed to H.Y.

Reprints and permissions information is available at www.nature.com/reprints.

Publisher's note Springer Nature remains neutral with regard to jurisdictional claims in published maps and institutional affiliations.

Open Access This article is licensed under a Creative Commons Attribution-NonCommercial-NoDerivatives 4.0 International License, which permits any non-commercial use, sharing, distribution and reproduction in any medium or format, as long as you give appropriate credit to the original author(s) and the source, provide a link to the Creative Commons licence, and indicate if you modified the licensed material. You do not have permission under this licence to share adapted material derived from this article or parts of it. The images or other third party material in this article are included in the article's Creative Commons licence, unless indicated otherwise in a credit line to the material. If material is not included in the article's Creative Commons licence and your intended use is not permitted by statutory regulation or exceeds the permitted use, you will need to obtain permission directly from the copyright holder. To view a copy of this licence, visit http://creativecommons.org/licenses/by-nc-nd/4.0/.

© The Author(s) 2025